Idle Speed Control of a Lean Burn Direct Injection Spark Ignition Engine

Julia Buckland, Ford Motor Company, Dearborn, MI [1]
J. W. Grizzle, University of Michigan, Ann Arbor, MI [2]

Abstract

Idle speed control is investigated for a direct injection, spark ignition, lean burn engine. The controller is designed to regulate engine speed, air-fuel ratio, exhaust gas recirculation and spark to desired set-points, whenever all set-point objectives are simultaneously achievable. Speed control becomes the primary objective when system constraints prohibit the simultaneous achievement of all goals. Novel features include the use of fuel as the primary fast torque actuator, instead of spark, and electronic throttle as a secondary actuator for torque.

1 Introduction

In recent years, many research and development activities have focused on achieving fuel economy improvements in spark ignition engines through reduced pumping losses [2, 8, 10, 1, 5]. One such technology is the direct injection stratified charge (DISC) gasoline engine. Its recent introduction into the Japanese and European markets may extend to North America in response to increased environmental pressures and higher customer expectations for fuel economy and performance. Capable of operating at air-fuel ratios of 40:1 to 50:1, the DISC engine has potential for significant benefits in fuel economy and CO_2 emissions. Since the improvements are the result of reduced pumping losses during lean operation, the fuel economy benefit is substantial at low engine speeds and torques, including typical idle speed conditions. Thus speed control during ultra lean operation is an important element of efficient DISC engine operation.

This paper addresses the problem of speed control for a lean burn engine equipped with an electronic throttle. In this context, speed control includes engine speed regulation and disturbance rejection tasks during idle operation [4, 12, 11]. The characteristics of lean burn engines are very different from conventional stoichiometric engines, creating new opportunities for improved speed control. In particular, air-fuel ratio is not constrained to a fixed value due to emissions considerations and is free to vary over a fairly wide range. Therefore, fuel may be used as the primary fast torque actuator instead of spark. Spark can then be set for maximum brake torque (MBT) to enhance fuel economy. The electronic throttle becomes a secondary actuator for torque, and is used when fuel must be limited due to air-fuel ratio constraints governed by combustion stability or soot formation.

This paper analyzes a simplified version of the speed control problem. Its purpose is to focus on the interactions of throttle and fuel as torque actuators, the impact of saturation on the controller design, and the interplay of speed control and fuel economy as performance objectives. The following assumptions will be made:

A1: Spark is set to achieve MBT.

A2: The range of allowable air-fuel ratios is continuous, varying from a minimum of stoichiometry to a maximum of 40:1.

A3: The changes in the intake manifold dynamics due to temperature variations can be handled through gain scheduling and robust control design, and thus a nominally constant temperature may be assumed.

A4: There is a fixed point in the cycle at which fuel injection quantity is determined. Thus, even though best fuel injection timing will naturally vary as a function of engine conditions, the combined computation delay and fuel injection delay is constant in terms of crank angle.

[1] J. Buckland is with the Powertrain Control Systems Department, Ford Research Laboratory, 2101 Village Road, PO Box 2053, Dearborn, MI 48121-2053. Email: jbucklan@ford.com

[2] J.W. Grizzle is with the Control Systems Laboratory, Electrical Engineering and Computer Science Department, University of Michigan, Ann Arbor, MI 48109-2122. Email: grizzle@umich.edu. His work was supported in part by NSF Grant ECS-9631237.

The controller is designed to regulate engine speed and achieve desired engine set-points whenever all objectives are feasible. When air-fuel ratio limits prohibit the control of torque via fuel, the controller performs speed regulation via the throttle, maintains the air-fuel ratio within allowed limits, and holds the intake manifold burned gas fraction at a desired value. Controller execution will be demonstrated with simulation results using a nonlinear model.

2 Lean Burn Engine Model

The engine analyzed is 1.8L with four cylinders. The engine model employed here is obtained by extrapolating the stratified charge mode of the DISC model of [9] to the full (continuous) range of allowed air-fuel ratios. Assumption A1 is very natural for fuel economy reasons and simplifies the torque expressions. Assumption A2 means that, for a DISC engine, the results presented here need to be supplemented to handle the disallowed range of air-fuel ratios, typically 20:1 to 25:1, where stable combustion is not achievable. Such a dead-zone is known to further complicate the control design. Assumption A3 simplifies the representation of the intake manifold dynamics and is straightforward to remove. Assumption A4 is reasonable from the perspective of real-time code execution.

With these assumptions, the air-charge, exhaust gas recirculation (EGR) and torque aspects of the engine are modeled as [9]

$$\begin{aligned} \dot{P}_i(t) &= \tfrac{RT_i}{V}\left(W_{th}(t)+W_{egr}(t)-W_{cyl}(t)\right) \\ \dot{m}_{bg}(t) &= F_e(t)W_{egr}(t)-F_i(t)W_{cyl}(t) \\ \dot{N}(t) &= \tfrac{1}{J_e}\left(\mathcal{T}_i(t-d)+\mathcal{T}_{fric}(t)-\mathcal{T}_{load}(t)\right), \end{aligned} \tag{1}$$

where P_i is the intake manifold pressure; R is the ideal gas constant; T_i is the intake manifold temperature; V is the intake manifold volume; W is a mass flow rate, with subscripts th, egr and cyl representing primary throttle, EGR and in-cylinder, respectively; m_{bg} is the mass of burned gas in the intake manifold; F_i and F_e are the burned gas fractions of the intake and exhaust manifolds, respectively; N is engine speed; J_e is engine inertia and $\mathcal{T}$ is torque, with subscripts i, $fric$ and $load$ representing the indicated, combined mechanical friction and pumping loss, and load torques, respectively.

These equations are completed by the following expressions:

$$\begin{aligned} d &= \tfrac{60}{N} \quad \text{one engine revolution} \\ W_{cyl} &= \alpha(N)+\beta(N)P \\ \mathcal{T}_i &= a_0(N)(1-F_i)W_{cyl}+a_1(N)W_f \\ \mathcal{T}_{fric} &= f(P_i,N) \\ F_i &= \tfrac{m_{bg}}{m_i} \\ m_i &= \tfrac{V}{RT_i}P_i \end{aligned} \tag{2}$$

where W_f denotes fuel flow rate and m_i corresponds to the mass of gas in the intake manifold. The parameters α, β, a_0 and a_1 are coefficients obtained via regression of engine mapping data.

The air-fuel ratio in the cylinder is given by

$$r_c = \frac{(1-F_i)W_{cyl}}{W_f}. \tag{3}$$

In addition, the air-fuel ratio and burned gas fraction of the exhaust can be computed to be

$$r_e = \frac{F_i W_{cyl}\frac{S}{S+1}+(1-F_i)W_{cyl}}{F_i W_{cyl}\frac{1}{S+1}+W_f} \tag{4}$$

$$F_e = \frac{S+1}{r_e+1}, \tag{5}$$

where $S = 14.64$ is the stoichiometric air-fuel ratio. The expressions for F_e and r_e are valid as long as $r_e \geq S$.

The mass air flow rate through the primary throttle valve, W_{th}, and the mass exhaust gas flow rate through the EGR valve, W_{egr}, are modeled with standard orifice flow equations [3] and any throttle dynamics have been ignored. Here, it is further assumed that the primary throttle has been feedback linearized via precompensation and hence can be represented by a model of the form

$$W_{th} = \mathrm{sat}_b^a(W_{th}^{des}) = \begin{cases} a & W_{th}^{des} \leq a \\ W_{th}^{des} & 0 < W_{th}^{des} < b \\ b & W_{th}^{des} \geq b \end{cases} \tag{6}$$

where

$$\begin{aligned} a &= 0 \\ b &= \frac{A_{th}(90)P_{amb}}{\sqrt{T_{amb}}}\phi\left(\frac{P_i}{P_{amb}}\right), \end{aligned}$$

$$\begin{aligned} \phi(x) &= \begin{cases} 4.04\times 10^4 & \text{if } x \leq 0.53 \\ 1.56\times 10^5\sqrt{(x^{1.4286}-x^{1.7143})} & \text{if } x > 0.53 \end{cases} \\ x &= \frac{P_i}{P_{amb}}. \end{aligned}$$

W_{th}^{des} is the desired mass air flow rate through the primary throttle and $A_{th}(90)$ is the throttle area corresponding to fully open throttle. Modeling errors will

result in (6) being only approximately true. However, such errors should be well within the gain margins of any of the controllers proposed here. Moreover, the pre-compensator could be adapted on the basis of available measurements [7].

EGR flow is modeled with a standard orifice equation,

$$W_{egr} = \frac{A_{egr}(\text{steps})P_e}{\sqrt{T_{egr}}}\phi\left(\frac{P_i}{P_e}\right), \qquad (7)$$

where A_{egr} is the EGR valve area, steps is the number of counts for positioning the stepper motor controlling the valve, P_e is the exhaust manifold pressure and T_{egr} is the temperature of the recirculated exhaust gas.

3 Idle Speed Control in the Absence of Air-Fuel Ratio Bounds

This section looks at idle speed control when fuel is the primary actuator. This is the case as long as adequate torque can be generated with air-fuel ratios between stoichiometry and 40:1 (Assumption A2). Section 4 studies the situation when air-fuel ratio constraints impose limits on fuel flow, in which case the throttle must be re-assigned for speed control.

3.1 Speed control based on fuel

Suppose for the moment that brake torque, $\mathcal{T}_b(t) := \mathcal{T}_i(t) + \mathcal{T}_{fric}(t)$, can be directly controlled. Then the speed control problem amounts to designing a controller for the system

$$\dot{N}(t) = \tfrac{1}{J_e}(\mathcal{T}_b(t-d) + \mathcal{T}^{del}_{fric} - \mathcal{T}_{load}(t)) \qquad (8)$$

where $\mathcal{T}^{del}_{fric} := (\mathcal{T}_{fric}(t) - \mathcal{T}_{fric}(t-d))$. The quantity $\mathcal{T}^{del}_{fric}$ will be small as long as the closed-loop system's bandwidth is less than $2/d$, which gives a bound of approximately 20 rad/sec. Neglecting for now saturation, the term $\mathcal{T}^{del}_{fric}$, as well as assuming that the load torque is unknown, but constant, results in a standard linear control problem. In order to achieve zero steady state error for constant engine speed commands, a PID-controller is appropriate. Using classical frequency domain design techniques results in the controller

$$\begin{aligned}\mathcal{T}_b(t) &= C_0(s)(N_{des} - N)(t) \qquad (9)\\ &= \left(K_p + \frac{K_I}{s} + \frac{K_D s}{.02s+1}\right)(N_{des} - N)(t),\end{aligned}$$

with $K_P = 0.28$, $K_I = 0.17$ and $K_D = 0.0094$.

The Bode plot of (9) cascaded with (8) is shown in Figure 1. For the purposes of computing the Bode plot, the time delay in (8) was approximated by a first order Padé approximation. The controller yields a gain crossover frequency of 7 rad/sec, a gain margin of 12 dB and a phase margin of 57 degrees. The controller is valid for any speed-torque point of the engine's operation. The closed-loop bandwidth is dictated by the time-delay, d.

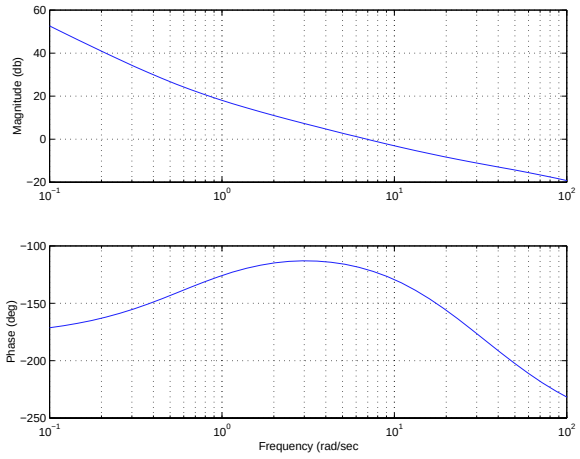

Figure 1: The Bode plot of (9) cascaded with (8).

Of course, brake torque is not directly controllable. In order to obtain an implementable controller, the control signal (9) is first related to indicated torque via

$$\mathcal{T}_i^{fuel}(t) := C_0(s)(N_{des} - N)(t) - T_f(t), \qquad (10)$$

and then to commanded fuel flow by

$$W_f(t) = \frac{T_i^{fuel}(t) - T_f(t) - a_0(N(t))(1 - F_i(t))W_{cyl}(t)}{a_1(N(t))}. \qquad (11)$$

The controller (11) can be applied as long as the air-fuel ratio stays within allowable bounds, such as stoichiometry to 40:1. For the moment, this is assumed to be the case, and attention is now turned to how to control the primary throttle and EGR valve in order to maintain desired set-points of air-fuel ratio and burned gas fraction. This will allow intermediate speed control simulations to be constructed. Then, the case of the fuel controller (11) resulting in an air-fuel ratio that is outside of the allowed bounds will be addressed.

3.2 Achieving EGR and air-fuel ratio set-points

Speed control must be integrated into a supervisory controller, which for given speed and load torque conditions, is charged with determining the optimal spark, EGR and air-fuel ratio settings for fuel economy and emissions [6]. Since the current speed control analysis assumes MBT spark, the remaining variables to be

controlled are EGR and air-fuel ratio. (Alternately, intake manifold pressure could be selected as the control variable instead of air-fuel ratio). Since fuel is being used to regulate engine speed, that leaves throttle as the actuator for air-fuel ratio.

The recirculated exhaust gas of a lean burn engine contains air as well as burned gas. For this reason, it is convenient to think of $W_{th} + W_{egr}$ as $W_{air} + W_{bg}$, where $W_{bg} = F_e W_{egr}$ is the mass flow rate of recirculated burned gas and $W_{air} = W_{th} + (1 - F_e)W_{egr}$ is the combined mass flow rate of air from the throttle and recirculated exhaust gas. Once the EGR flow rate has been set, the primary throttle command is then determined by $W_{th}^{des} = W_{air}^{des} - (1 - F_e)W_{egr}$, where W_{air}^{des} is the desired mass air flow rate. Of course, there will be inevitable inaccuracies in the estimation of W_{egr} and F_e, and hence in the determination of W_{th}^{des}. This must be compensated for by robustness of the control design.

EGR control is typically implemented in a feedforward (open-loop) manner, and this approach was followed here as well. The exhaust manifold was assumed to be nominally at 101 KPa and 500 K. Based on these nominal values, the method given in [7] was used to maintain the intake manifold burned gas fraction at a desired level. Here, the set-point was chosen to be $F_i = 0.1$.

In order to simplify vehicle calibration, it is desirable that the throttle to air-fuel ratio controller be as independent as possible of the fuel to speed controller, whenever the speed disturbances can be handled by fuel flow rate adjustments alone. For these two controllers to be "independent," a good rule of thumb is to keep the bandwidths of their respective closed-loop systems a decade or so apart. Since the fuel to speed control loop has a bandwidth of 7 rad/sec, it follows that the bandwidth of the throttle to air-fuel ratio loop should be upper bounded by 0.7 to 1 rad/sec. It turns out that the long delay in the measurement of r_e essentially imposes that the bandwidth of the throttle to air-fuel ratio feedback loop be no faster than one radian per second in any case.

Assuming that exhaust air-fuel ratio can be measured accurately under ultra lean conditions, (4) can be used to obtain an equivalent cylinder mass flow rate estimate by

$$W_{cyl} = \frac{W_f}{1 - F_i \frac{r_e+1}{S+1} r_e}. \qquad (12)$$

This can be used to replace the air-fuel ratio control problem with one of designing a set-point controller for the system

$$\begin{aligned} \dot{P}_i &= \frac{RT_i}{V}(W_{air} - W_{cyl}) \qquad (13) \\ y &= W_{cyl}(t - 3d) \end{aligned}$$

Classical design rules lead to the PI controller

$$W_{air}(t) = (K_P^1 + \frac{K_I^1}{s})(y^{des}(t) - y(t)), \qquad (14)$$

with $K_P^1 = 2/3$ and $K_I^1 = 1$. The associated Bode loop gain is shown in Figure 2.

Remark: The advantage of working with (12) instead of $(r_e^{des} - r_e)(t)$ is that (12) automatically schedules the controller gains as a function of engine operating points. Also, in practice, one may not wish to rely on measured r_e since it may be quite inaccurate at very lean air-fuel ratios. Using (12), the controller can be implemented on the basis of estimated quantities. Here, the controller (14) was implemented as

$$W_{air}(t) = (K_P^1 + \frac{K_I^1}{s})(\frac{W_f(t - 3d) r_e^{des}}{1 - \hat{F}_i(t - 3d)\frac{r_e^{des}+1}{S+1}} - \hat{W}_{cyl}), \qquad (15)$$

where $\hat{F}_i$ and $\hat{W}_{cyl}$ were estimated via an observer.

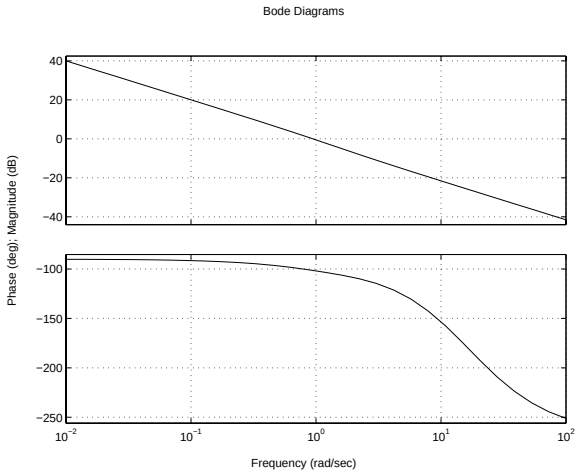

Figure 2: Bode plots for the cascade of the controller (14) with the system (13).

3.3 Intermediate simulations

Figure 3 shows the response of the closed-loop system to a step in engine load (accessory) torque of 15 Nm. It is seen that without any feedforward information on the load step, the speed droops to approximately 700 RPM from the assumed set-point of 750 RPM. The rapid torque response is obtained by decreasing the air-fuel ratio to 22:1 from the assumed optimal value of 30:1 at a load torque of 10 Nm. The throttle to air-fuel ratio controller then moves the air-fuel ratio back to the assumed optimal position. This

was possible because the load was sufficiently small that the commanded air-fuel ratio could be achieved with the manifold pressure less than atmospheric.

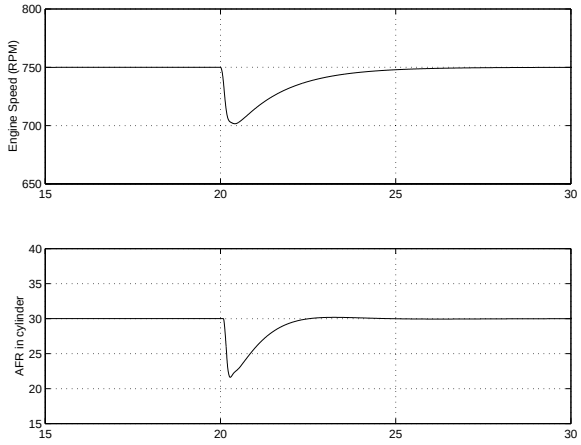

Figure 3: Torque step from 10 Nm to 25 Nm applied at time 20 seconds. EGR set-point of $F_i = 0.1$ and AFR set-point of 30:1.

4 Speed Control in the Presence of Air-Fuel Ratio Bounds

In response to a sufficiently large added load torque, the controller (11) will command a value of fuel that will result in an air-fuel ratio that exceeds a desired lower bound, R_1, say stoichiometry. Also, in response to the removal of a sufficiently large load, it will command a value of fuel resulting in an air-fuel ratio that is higher than an allowable upper bound, R_2, say the lean limit. In either case, the fuel flow rate, as an actuator, is effectively saturated. If speed control is of higher priority than set-point optimality, as is the case for idle speed control, then the throttle must be re-assigned for speed control. This section develops a throttle controller to be used for speed regulation when the fuel saturates.

4.1 Dynamic effects of EGR

Since the idle speed control loop needs to be as responsive to load disturbances as possible, the controller design needs to maximize bandwidth, subject to preserving robustness to model uncertainty. At an air-fuel ratio of 35:1, achieving a burned gas fraction of 0.1 in the intake manifold requires about two and half times more recirculated exhaust gas than when the air-fuel ratio is at stoichiometry. Hence, a key element in understanding the system dynamics from throttle to engine speed is the effect of EGR on the intake manifold (or air charge) dynamics.

Linearizing the orifice flow equation for the EGR valve about a nominal operating point results in

$$W_{egr} \approx b_0(steps) + b_1(steps)P_i \tag{16}$$

where steps represents EGR valve position, which is measured in steps. It is important to understand how the coefficients b_0 and b_1 vary with engine operating condition. The value of b_1 is of particular interest because it will directly affect system dynamics. Assuming P_i is limited[1] to 95 kPa, the minimum value of b_1 occurs when the valve is wide open, yielding $b_{1\ min} = -0.5$. The maximum value occurs when the EGR valve is closed or flow is choked, yielding $b_{1\ max} = 0$.

Given this representation of W_{egr} and the expression for W_{cyl} from (2), a block diagram of the intake manifold dynamics can be constructed and is illustrated in Figure 4. The delay element, $e^{-d_e s}$, represents an estimated time required for the mass flow rate of recirculated exhaust gas to respond to changes in intake manifold pressure. The plant model needed for control development is given by the transfer function from W_{th} to W_{cyl}. Using a first order Padé approximation to represent the time delay, this transfer function is given by

$$W_{cyl}(s) = \frac{\frac{RT_i}{V}\beta(s + \frac{2}{d_e})}{s^2 + [\frac{2}{d_e} + \frac{RT_i}{V}(\beta + b_1)]s + \frac{RT_i}{V}\frac{2}{d_e}(\beta - b_1)} W_{thr}(s) \tag{17}$$

Thus the model parameters b_1 and β affect the natural frequency and damping of the system. The range of values of b_1 and β are such that the system is always critically damped. Consequently, variation in these parameters will primarily affect the bandwidth of the system. This is illustrated with Bode plots of (17), shown in Figure 5. Plots are shown for each combination of minimum and maximum parameter values. All realistic plants will fall within these boundaries. Therefore, the controllers developed to actuate the throttle must be robust to model uncertainty within these bounds.

4.2 Throttle-based control of speed

Let $[R_1, R_2]$ be the allowed range of air-fuel ratios. Assume that W_f has been limited to meet the air-fuel ratio bounds, so that $W_f = \frac{(1-F_i)W_{cyl}}{R_j}$, where $j \in \{1, 2\}$. Then torque is determined by air flow. On this basis, the indicated torque can be re-written as

$$\mathcal{T}_i = (a_0(N) + a_1(N)/R_j)(1 - F_i)W_{cyl} \tag{18}$$

[1] EGR flow rate goes to zero as intake manifold pressure approaches exhaust manifold pressure. Since (7) is not differentiable at $P_i = P_e$, linear analysis breaks down at that point.

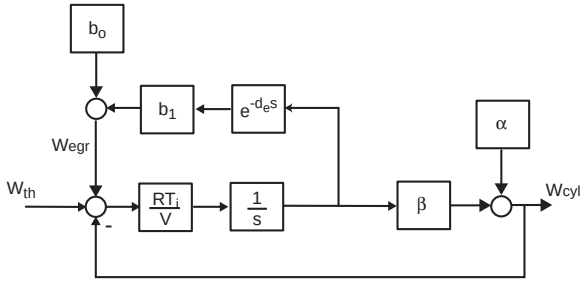

Figure 4: Block diagram of intake manifold system with EGR.

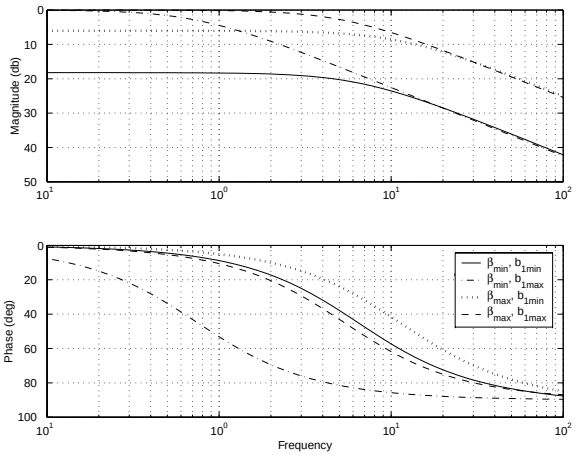

Figure 5: Bode plots of Intake Manifold System with model parameter variations due to EGR.

and solved for W_{cyl} in order to obtain the desired mass flow rate of air out of the intake manifold as a function of desired indicated torque. The question at hand can be viewed as one of determining a proper controller for the throttle so that this is achieved.

Figure 6 depicts the controller architecture employed for regulating speed via the throttle when fuel is saturated based on air-fuel ratio constraints. The structure of the controller is highly suggestive of an inner-outer loop design from classical control. This structure allows throttle-based speed control to be integrated with the fuel-based speed controller, (9), (10) and (11), with considerable ease, as will be seen.

Linear time-invariant compensators $C_1(s)$ and $C_2(s)$ were designed on the basis of classical frequency domain design rules. Figure 7 displays the loop gain from speed error, $N^{des} - N$, to N for the compensators

$$C_1(s) = \frac{(1.2s+1)}{0.02s+1} C_0(s) \quad (19)$$

$$C_2(s) = 0.086 \quad (20)$$

Note that $C_1(s)$ is factored into the fuel PI controller of (10), cascaded with a lead term. The DC gain of the lead term has been deliberately set to 1.0 and the overall loop gain adjusted with $C_2(s)$. The purpose of the lead term is to compensate for the phase lag due to the manifold filling dynamics. The form (19) makes it natural to take the output of the fuel-based speed controller and pass it through the lead term $\frac{(1.2s+1)}{0.02s+1}$ in order to compute the commanded indicated torque for the throttle-based speed controller. From this, it is clear that there is only one integrator that will have to be protected by anti-windup logic.

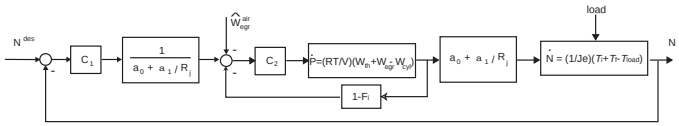

Figure 6: Speed controller architecture when fuel is saturated and throttle is the primary actuator.

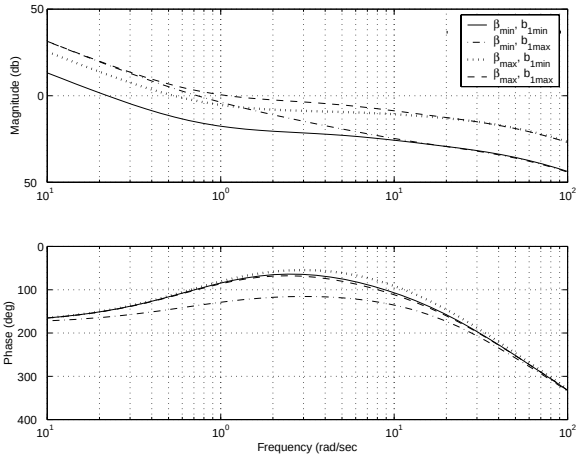

Figure 7: Bode plots for the throttle based speed control cascaded with the engine model for the two extremes of model variations due to EGR.

The speed-throttle controller should only be active when the speed-fuel controller results in saturation of the fuel actuator. This is conveniently achieved in the following manner. Define

$$\hat{r}_c(t) := \frac{(1 - F_i(t-d))W_{cyl}(t-d)}{W_f(t-d)}, \quad (21)$$

which is the current (estimated) in-cylinder air-fuel ratio. Define

$$R(t) := \begin{cases} R_1 & \hat{r}_c(t) \le R_1 \\ \hat{r}_c(t) & R_1 < \hat{r}_c(t) < R_2 \\ R_2 & \hat{r}_c(t) \ge R_2 \end{cases}, \quad (22)$$

and

$$W_{cyl}^{T_i} = \frac{T_i^{th}}{a_0 + a_1/R}. \tag{23}$$

Then

$$W_{th}^{T_i} = C_2(s)(1 - F_i)(W_{cyl}^{T_i} - W_{cyl}) \tag{24}$$

will be asymptotically zero when the estimated in-cylinder air-fuel ratio is strictly within the allowable bounds given by R_1 and R_2, and will implement the speed-throttle controller otherwise. Indeed, from (10) and (11), and (21)-(23), it follows that as long as the DC-gain of $\frac{C_1(s)}{C_0(s)}$ equals one, then

$$\lim_{t\to\infty}(W_{cyl}^{T_i} - W_{cyl})(t) = 0 \tag{25}$$

under steady state conditions. Recall that, by design, $\frac{C_1(s)}{C_0(s)} = \frac{(1.2s+1)}{0.02s+1}$ has a DC-gain of unity.

4.3 Introducing nonlinearities and logic to deal with saturation

Several more issues must be addressed before the compensators (9), (15), (19) and (20) can be integrated into a functional speed controller. Each issue is a direct or indirect consequence of saturation.

Issue-1: The engine produces limited indicated torque, whereas (9) and (19) implicitly assume that $\mathcal{T}_i$ is not bounded from above or below. When the engine is producing its maximum or minimum torque, anti-windup logic must be placed around the integrator in (9).

Issue-2: The overall speed controller must deal with at least two modes of operation. In the first mode, both fuel and throttle are unsaturated, and consequently, both speed and optimal set-point objectives can be pursued by the controller. In this mode, it is still possible that the planned set-point cannot be achieved due to the manifold pressure reaching its maximum. Anti-windup logic is thus necessary around the integrator of (15). In the second mode, fuel is saturated, and only the speed objective can be pursued. The transition between these two modes must be addressed. This includes when to activate the integrator in (15) and when to de-activate it.

Issue-3: Since indicated torque is non-negative, the removal of a large load can result in significant speed 'flare', followed by speed undershoot, unless a 'dashpot' type of action is incorporated into the controller.

The modifications to the basic controller are illustrated in Figure 8. Details of the implementations are not provided due to limited space.

4.4 Illustrative simulation

Figure 9 depicts the concerted action of the controllers (9), (15), (19) and (20) when a 35 Nm load is suddenly applied to the system, with no feedforward action. It is remarkable that the closed-loop system can deal with such a large disturbance with no feedforward control and only result in a speed droop of 115 RPM. The effects of the sudden removal of the load are somewhat more dramatic, resulting in a speed flare of 175 RPM. The controller uses rapid engine braking to bring the speed back to within 2% of the nominal 750 RPM set-point in about 2 seconds. Note that at this operating condition, the throttle is effectively saturated since the intake manifold pressure is near atmospheric. Consequently, the system cannot achieve the AFR set-point of 30:1 with $F_i = 0.1$.

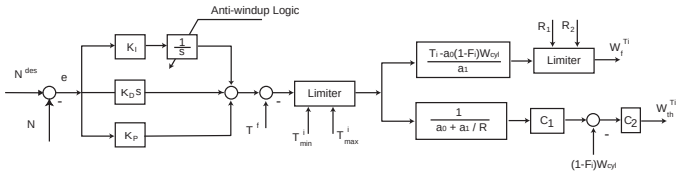

Figure 8: Schematic representation of the modifications to the basic speed controller.

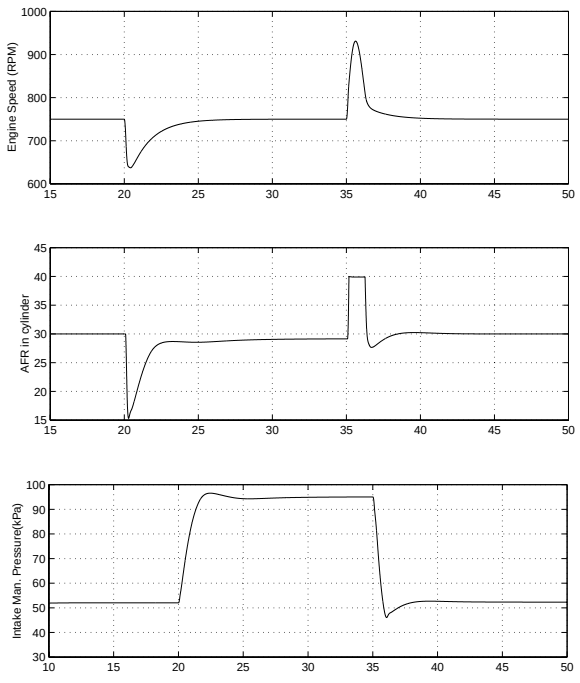

Figure 9: Torque step from 10 Nm to 45 Nm applied at time 15 seconds and removed at 30 seconds. EGR set-point of $F_i = 0.1$ and AFR set-point of 30:1.

4.5 Extension to cruise control

With the addition of a vehicle model, the control ideas presented above can be applied to cruise control as well. Figure 10 illustrates the response of the control system to a step in commanded speed set-point from 750 RPM to 2000 RPM at time 20 seconds, and back to 750 RPM at time 35 seconds. The load was held constant at 10 Nm. The only change in the control scheme is the addition of a speed command pre-filter, which allows speed errors due to speed set-point command changes to be treated differently than speed errors due to load disturbances. Note that there is no overshoot or undershoot, even at this light load. The lack of overshoot on a step increase in speed is largely due to the two-degree of freedom control design. The lack of undershoot is primarily due to the judicious regulation of intake manifold pressure by the dashpot mode.

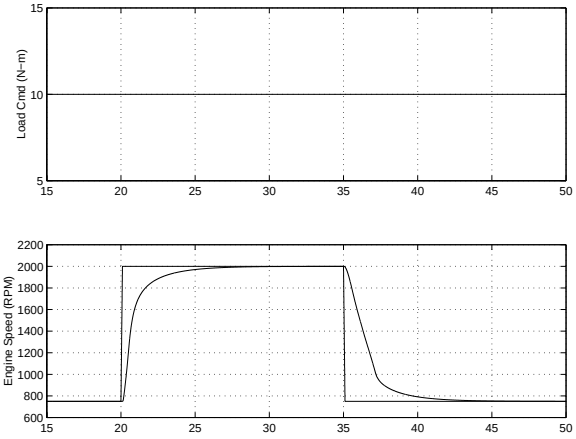

Figure 10: Speed step up to 2000 RPM and back down to 750 RPM, at 10 Nm load.

References

[1] M. S. Ashhab, A. G. Stefanopoulou, J. A. Cook, and M. Levin. Camless engine control for robust unthrottled operation. *SAE Paper*, (981031), 1998.

[2] A. C. Elrod and M.T. Nelson. Development of a variable valve timing engine to eliminate the pumping losses associated with throttled operation. *SAE Paper*, (860537), 1986.

[3] J. B. Heywood. *Internal Combustion Engine.* McGraw-Hill, 1988.

[4] Devor Hrovat and Jing Sun. Models and control methodologies for IC engine idle speed control design. *Control Engineering Practice*, 5(8):1093–1100, 1997.

[5] J. Kang and J.W. Grizzle. Nonlinear control for joint air and fuel management in a SI engine. In *Proc. Amer. Contr. Conf., San Diego*, 1999.

[6] J.M. Kang, I. Kolmanovsky, and J.W. Grizzle. Approximate dynamic programming solutions for lean burn engine aftertreatment. In *IEEE Conference on Decision and Control, Phoenix, AZ*, 1999.

[7] I. Kolmanovsky, J. Sun, M. Druzhinina, and M. van Nieuwstadt. Charge control for direct injection spark ignition engines with EGR. In *Proceedings of the American Control Conference, Chicago, IL*, 2000.

[8] T. G. Leone, E. J. Christenson, and R. A. Stein. Comparison of variable camshaft timing strategies at part load. *SAE Paper*, (960584), 1996.

[9] J. Sun, I. Kolmanovsky, D. Brehob, J.A. Cook, J. Buckland, and M. Haghgooie. Modeling and control of gasoline direct injection stratified charge (DISC) engines. In *International Conference on Control Applications*, 1999.

[10] O. Vogel, K. Roussopoulos, L. Guzzella, and J. Czekaj. Variable valve timing implemented with a secondary valve on a four cylinder SI engine. *1997 Variable Valve Actuation and Power Boost SAE Special Publications*, 1258(970335):51–60, February 1997.

[11] Yan Wang, Anna Stephanopoulou, and Mike Levin. Idle speed control: an old problem in a new engine design. In *Proc. Amer. Contr. Conf., San Diego*, pages 1217–1221, 1999.

[12] S. Yurkovich and M. Simpson. Comparative analysis for idle speed control: a crank-angle domain viewpoint. In *Proc. Amer. Contr. Conf., New Mexico*, pages 278–283, June 1997.